NEOPLASIA
www.neoplasia.com

Volume 16 Number 5 May 2014 pp. 451–460 451

CEACAM1 Promotes Melanoma Cell Growth through Sox-2[1,2]

Rona Ortenberg*,†, Gilli Galore-Haskel*,†, Ilanit Greenberg*, Bella Zamlin*,†, Sivan Sapoznik*, Eyal Greenberg*,†, Iris Barshack‡, Camila Avivi‡, Yulia Feiler§, Israel Zan-Bar†, Michal J. Besser*,†, Ester Azizi¶, Friedman Eitan#, Jacob Schachter*,3 and Gal Markel*,†,,3**

*Ella Institute of Melanoma, Sheba Medical Center, Ramat-Gan, Israel; †Department of Clinical Microbiology and Immunology, Sackler Faculty of Medicine, Tel Aviv University, Tel Aviv, Israel; ‡Institute of Pathology, Sheba Medical Center, Ramat-Gan 526260, Israel; §Cancer Research Center, Sheba Medical Center, Ramat-Gan, Israel; ¶Department of Dermatology, Sheba Medical Center, Ramat-Gan, Israel; #The Susanne-Levy Gertner Oncogenetics Unit, Danek Gertner Institute of Human Genetics, Ramat-Gan, Israel; **Talpiot Medical Leadership Program, Sheba Medical Center, Ramat-Gan, Israel

Abstract

The prognostic value of the carcinoembryonic antigen cell adhesion molecule 1 (CEACAM1) in melanoma was demonstrated more than a decade ago as superior to Breslow score. We have previously shown that intercellular homophilic CEACAM1 interactions protect melanoma cells from lymphocyte-mediated elimination. Here, we study the direct effects of CEACAM1 on melanoma cell biology. By employing tissue microarrays and low-passage primary cultures of metastatic melanoma, we show that CEACAM1 expression gradually increases from nevi to metastatic specimens, with a strong dominance of the CEACAM1-Long tail splice variant. Using experimental systems of CEACAM1 knockdown and overexpression of selective variants or truncation mutants, we prove that only the full-length long tail variant enhances melanoma cell proliferation *in vitro* and *in vivo*. This effect is not reversed with a CEACAM1-blocking antibody, suggesting that it is not mediated by intercellular homophilic interactions. Downstream, CEACAM1-Long increases the expression of Sox-2, which we show to be responsible for the CEACAM1-mediated enhanced proliferation. Furthermore, analysis of the CEACAM1 promoter reveals two single-nucleotide polymorphisms (SNPs) that significantly enhance the promoter's activity compared with the consensus nucleotides. Importantly, case-control genetic SNP analysis of 134 patients with melanoma and matched healthy donors show that patients with melanoma do not exhibit the Hardy-Weinberg balance and that homozygous SNP genotype enhances the hazard ratio to develop melanoma by 35%. These observations shed new mechanistic light on the role of CEACAM1 in melanoma, forming the basis for development of novel therapeutic and diagnostic technologies.

Neoplasia (2014) 16, 451–460

Introduction

Melanoma accounts for nearly 4% of all skin cancers, and it causes 75% of skin cancer–related deaths worldwide. Estimates for 2013 are that 76,690 invasive melanomas will be diagnosed in the United States and that melanoma could claim 9480 lives. Melanoma is the fifth most common cancer in men and seventh in women in the United States [1]. Disease progression and development of metastasis require stepwise acquisition of aggressive characteristics [2], including resistance to the immune system

Address all correspondence to: Dr Gal Markel, Ella Institute of Melanoma, Sheba Medical Center, Ramat-Gan 526260, Israel. E-mail: markel@post.tau.ac.il

[1] This research was funded by a grant from the Israel Cancer Research Fund (Research Career Development Award).

[2] This article refers to supplementary materials, which are designated by Tables W1 to W4 and Figures W1 to W4 and are available online at www.neoplasia.com.

[3] These authors contributed equally to this work.

 1476-5586/14
http://dx.doi.org/10.1016/j.neo.2014.05.003

[3], even though melanoma cells are frequently immunogenic [4]. In the last years, the US Food and Drug Administration approved the anti-Cytotoxic T-Lymphocyte Antigen 4 monoclonal antibody (mAb) (ipilimumab), the selective $BRAF^{V600E}$ inhibitors vemurafenib and dabrafenib, as well as the mitogen-activated protein kinase kinase enzymes (MEK) inhibitor trametinib for the indication of metastatic melanoma. Although these drugs show proven benefit in overall survival [4–6], the treatment for melanoma is still far from being satisfactory.

Carcinoembryonic antigen cell adhesion molecule 1 (CEACAM1) is a transmembrane glycoprotein that belongs to the carcinoembryonic antigen family, which encompasses several forms of proteins with different biochemical properties, all encoded on chromosome 19 [7]. CEACAM1 is composed of sequentially ordered extracellular immunoglobulin-like domain(s), a single-pass transmembrane domain, and a cytoplasmic tail. Different transcriptional splice variants give rise to several isoforms, which differ in the number of Ig-like domains at the extracellular N terminus, the length of the cytoplasmic tail, and the presence of Alu repeats. The most common and sequenced variants are short and long forms of CEACAM1-3 and CEACAM1-4. A long form contains immunodominant tyrosine-based inhibitory motif (ITIM), and a short form is devoid of ITIM [7]. CEACAM1 interacts homophilically with CEACAM1 and heterophilically with CEACAM5, but not with other CEACAM proteins [8]. CEACAM1 is expressed on a variety of cells, e.g., some epithelial cells, melanoma, and activated lymphocytes [7].

Many different functions have been attributed to the CEACAM1 protein, including antiproliferative properties in carcinomas of the colon and prostate and central involvement of CEACAM1 in angiogenesis and insulin clearance as well as in immune-modulation {reviewed in [7,9]}. T cell inhibition through engagement of CEACAM1 has been demonstrated by direct T cell receptor cross-linking [10] and through binding of *Neisseria* opacity-associated proteins [11]. Inhibition is mediated through the recruitment of SHP-1 phosphatase to the cytosolic ITIM sequences [7]. We have previously shown that CEACAM1 homophilic interactions inhibit NK cell–mediated killing independently of major histocompatibility complex class I recognition [12–14]. We have further demonstrated that CEACAM1 inhibits cytotoxicity and interferon gamma (IFNγ) release of tumor-infiltrating lymphocytes [15]. Moreover, we found that an IFNγ-driven up-regulation of CEACAM1 on melanoma cells surviving tumor-infiltrating lymphocyte–mediated attack renders them even more resistant [16]. Following these findings, we developed a novel approach for melanoma immunotherapy, which is based on functional blocking of CEACAM1 with a specific mAb [17].

Thies et al. demonstrated that the presence of CEACAM1 on primary cutaneous melanoma lesions strongly predicted the development of metastatic disease [18]. This was in line with our findings that CEACAM1 protects melanoma cells and inhibits both activated NK cells [13] and activated T cells [15,16,19], emphasizing the potential role played by CEACAM1 in the pathogenesis of metastatic melanoma and justifying the development of a therapeutic approach that targets the function of CEACAM1 [17]. Nevertheless, the direct effect of CEACAM1 on the biology of melanoma cells, regardless of the immune-protective effect, has never been tested. This is particularly interesting in light of the following two points: 1) CEACAM1 expression predicts metastatic spread in melanoma xenograft models in immunodeficient mice [20]; and 2) CEACAM1 suppresses cell proliferation in other malignancies, such as colon [21] and prostate [22].

Here, we show that CEACAM1 is gradually upregulated during melanoma development and progression. It facilitates the proliferation of melanoma cells in a Sox-2–dependent manner. Two single-nucleotide polymorphisms (SNPs) found in the promoter region enhance its activity, and homozygosity increases the risk of developing melanoma by 35%. These observations highlight the direct pivotal role of CEACAM1 in melanoma.

Methods

Cells and Antibodies

We used melanoma American Type Culture Collection (ATCC) (Manassas, VA, USA) cell lines A375, G361, WM 115, SK MEL 5, SK MEL 28, MeWo, WM 266-4, National Institutes of Health (NIH) (Bethesda, MD, USA) cell lines 526mel and 624mel, as well as 40 primary cultures of metastatic melanoma [16,17]. All melanoma cells were grown in RPMI medium supplemented with 10% FBS, 100 μg/ml Pen/Strep, 2 mM L-Glutamine, 25 mM Hepes, and 1 mM sodium pyruvate (Biological Industries, Beit Ha-Emek, Israel) and incubated in 37°C, 5% CO_2 condition.

The antibodies used in this work are described in Table W1.

Flow Cytometry

MRG1, a homemade specific to CEACAM1 monoclonal mouse antibody [23], was used to determine surface CEACAM1 expression. A population of 100,000 cells was incubated with 0.1 μg of antibody diluted in FACS buffer [phosphate-buffered saline (PBS), 0.02% sodium azide, and 0.5% BSA] for 30 minutes on ice. After incubation, cells were centrifuged 400*g* at 4°C for 5 minutes, and supernatant was removed. Cells were then incubated on ice with Fluorescein isothiocyanate (FITC)-conjugated secondary antibody for 30 minutes, washed with FACS buffer, and analyzed with FACSCalibur instrument (BD bioscience, San Jose, CA, USA) and FlowJo software (Tree Star Inc, Ashland, OR, USA).

Cell Cycle

A population of 10^6 cells was pelleted, washed twice with PBS, and fixated with 70% ethanol overnight. Following fixation, cells were permeabilized with 0.05% Triton X (Sigma-Aldrich, Rehovot, Israel) and stained with 1 μg/ml propidium iodine (Sigma). The analysis was performed using a FACSCalibur instrument (BD Biosciences) and FlowJo software (Tree Star Inc).

Western Blot Analysis

A population of 5×10^6 cells was washed with PBS and lysed in radio immunoprecipitation assay buffer (RIPA) lysis buffer (Sigma) supplemented with protease inhibitor cocktail (Roche, Basel, Switzerland) on ice for 20 minutes. Insoluble material was removed by centrifugation at 14,000 rpm for 10 minutes at 4°C. Protein concentration was measured using Pierce BCA protein kit (Thermo Scientific, Waltham, MA, USA). Proteins were separated by 10% to 12% sodium dodecyl sulfate–polyacrylamide gel electrophoresis, transferred onto nitrocellulose membranes (Bio-Rad Laboratories, Hercules, CA, USA), and incubated with specific antibodies. The antigen-antibody complexes were visualized by standard enhanced chemiluminescence reaction (Biological Industries, Beit Ha-Emek, Israel).

Knockdown of CEACAM1

Generation of stable CEACAM1-silenced 526mel cells was performed using commercially available target sequences cloned in the MISSION short hairpin RNA system (lentiviral plasmids pLKO.1-

puro) (Sigma) and lentiviral expression system. Scrambled nontarget sequence was used as negative control.

Generation of transient CEACAM1-silenced melanoma cells was performed using commercially available Dharmacon siGENOME Human SMARTpool (Thermo Scientific) small interference RNA (siRNA) system. Cells were grown until 75% of the surface of the plate and transfected for 24 hours with either experiment CEACAM1-specific siRNA (10 nM) or nontargeting scramble siRNA as a negative control (10 nM) using jetPRIME reagent (Polyplus-transfection SA, Strasbourg, France) according to the manufacturer's instructions. After 24 hours, transfection mixtures were replaced with regular medium, and cells were maintained in normal culture condition before the experiments.

Generation of Constructs

The expression system used in this work was pQCXIP/puro. All fragments were subcloned into *Not*I/*Eco*RI sites. The various primers that were designed for cloning are provided in Table W2. To create the fusion proteins such as extracellular portion of CEACAM1 fused to glycosyl phosphoinositol (GPI) anchor (EC-GPI) and CEACAM1 transmembrane domain with long tail portions fused upstream to green fluorescent protein (GFP), preceded by the leader peptide of CEACAM1 (GFP-CT-L), the polymerase chain reaction (PCR)–driven overlap extension approach was used [23].

Generation of Viral Particles and Cell Transduction

Lentiviral or retroviral particles were produced by transient liposome-mediated cotransfection (TurboFect; Thermo Scientific) of 293 T cells with lentiviral or retroviral packaging plasmids and the vector containing the experimental construct. Culture medium was replaced 6 hours after transfection with fresh complete Dulbecco's modified Eagle's medium and incubated for an additional 42 hours. The medium containing viral particles was collected and filtered through a 0.45-μm filter. Previously seeded cells were infected two consecutive days (twice total) by the filtered virus-containing medium with 1 μg/ml polybrene. Virus-containing medium was replaced after 6 hours with fresh medium. Forty-eight hours after the second infection, selection antibiotic [puromycin (1 μg/ml)] was added into the culture medium.

Knockdown of Sox-2

siRNA-mediated gene knockdown Trilencer-27 siRNA kit (OriGene Technologies Inc, Rockville, MD) was used to downregulate SOX2 expression in 003mel/CCM1-L (CEACAM1-Long) cells. Cells were grown until 75% of the surface of the plate and transfected for 24 hours with either experiment SOX2-specific siRNA (10 nM) or nontargeting scramble siRNA as a negative control (10 nM) using jetPRIME reagent (Polyplus-transfection SA) according to the manufacturer's instructions. After 24 hours, transfection mixtures were replaced with regular medium, and cells were maintained in normal culture condition before the experiments.

RNA Isolation and Reverse Transcription

Total RNA was isolated using TRI Reagent (Sigma-Aldrich, Rehovot, Israel), according to the manufacturer's instructions. cDNA was generated by high-capacity reverse transcriptase kit (Applied Biosystems, Foster City, CA, USA) using random hexamer primers according to the manufacturer's instructions.

Quantitative Real-Time Reverse Transcription–PCR

Expression levels of different genes were determined by quantitative real-time reverse transcription–PCR (qRT-PCR). Primers (Sigma-Aldrich) were designed according to Primer Express software guidelines (Applied Biosystems). The qRT-PCR reactions were run in triplicate on LightCycler 480 system (Roche). Gene transcripts were detected using LightCycler 480 SYBR Green I Master (Roche). Reactions were normalized to Glyceraldehyde 3-phosphate dehydrogenase (GAPDH) endogenous control. The detailed list of primers used for qRT-PCR appears in Table W2.

Net Proliferation Assay

Melanoma cells (5×10^3) were seeded in triplicate wells in 96 F-well microplates. Net proliferation was determined by standardized (2,3-Bis-(2-Methoxy-4-Nitro-5-Sulfophenyl)-2H-Tetrazolium-5-Carboxanilide) (XTT) colorimetric assay, according the manufacturer's instructions (Biological Industries).

Progression Tissue Microarray and Immunohistochemistry

Tissue Micro-Array (TMA) slides were provided by the National Cancer Institute (NCI) (Bethesda, MD, USA) Cancer Diagnosis Program and included 66 benign nevi, 90 primary tumors, and 74 metastases. Other investigators may have received slides from these same array blocks. This study was approved by the Institutional Review Board. TMAs were stained with standard protocols with mAb MRG1 as described [17] and analyzed by an expert pathologist. Intensity of CEACAM1 expression was scored from 0 (negative) to 3, and percentages of expression were defined as 0 to 3 for 0% to 5%, 6% to 25%, 26% to 75%, and 76% to 100%, respectively. The entire tissue cylinder from each case was evaluated.

Melanoma Xenograft Model

Melanoma cells (2×10^6) were injected subcutaneously to the thigh of 7- to 8-week-old Severe Combined Immunodeficiency/Nonobese Diabetic (SCID-NOD) mice to create human melanoma xenografts. Mice were monitored three times per week for tumor volume by caliper measurement. Tumor volume was calculated as: $(\text{small diameter})^2 \times (\text{large diameter})/2$. Each group included 8 to 10 mice. At the end of the experiment, the tumors were extracted and homogenized for further tests. All animal work was performed following approval of Sheba Medical Center Internal Regulatory Board (IRB) (434/2010).

Microarray Expression Analysis

Total RNA was extracted and used as template to generate cDNA and subsequent biotinylated target cRNA that was processed by an Affymetrix GeneChip Instrument System (Affymetrix, Santa Clara, CA, USA) according to the manufacturer's recommendations. The complete description of this procedure is available at: http://Affymetrix.com/support/technical/manual.affx. The Database of Essential Genes (DEGs) were analyzed by Ingenuity Pathway Analysis (Redwood City, CA, USA) (http://www.ingenuity.com).

Patients and Healthy Individuals

One hundred thirty-four patients with histopathologically confirmed melanoma, who attended the Dermatological Clinic at Sheba Medical Center from 2001 to 2008, were recruited. One hundred thirty-three ethnically matched normal individuals, who came to the same medical center during the same period for noncancer-related diseases, were recruited as control group (IRB Approval No. 4183/2006). All participants signed a written informed consent. DNA was extracted from venous blood leukocytes from all patients with melanoma and healthy individuals.

Selection of CEACAM1 SNPs and Genotyping

SNPs within the *CEACAM1* gene were selected from National Center for Biotechnology Information (NCBI), www.ncbi.nlm.nih.gov (Bethesda, Maryland) SNP database (http://www.ncbi.nlm.nih.gov/snp). Only SNPs in exons were evaluated. SNPs within the coding region that cause a synonymous change were excluded. Validation status and rate of polymorphisms in the tested population were taken into account. Genotyping was performed in 384-well microplates and determined by Matrix Assisted Laser Desorption Ionization Time-of-Flight (MALDI-TOF) Sequenom (Sequenom, San Diego, CA) platform as described previously [24]. Genotyping assays were designed as iPLEX reactions using SpectroDESIGNER software version 3.1 (Sequenom). The list of amplification and extension primers is provided in Table W3.

CEACAM1 Promoter Functional Tests

A DNA fragment containing the putative minimal promoter of CEACAM1 (600 bp upstream to CEACAM1 start codon), was amplified and cloned into pGL4.14 LUC reporter vector (Promega, Madison, WI) into *Xho*I/*Hind*III sites. Double mutations, mimicking CEACAM1 SNPs (rs8103285 and rs8102519), were inserted using QuikChange Multi Site-Directed Mutagenesis Kit (Stratagene, La Jolla, CA), according to manufacturer's protocol. Table W2 provides list of primers used for putative minimal promoter cloning and mutagenesis. Constructs and pRL *Renilla* Luciferase Reporter Vector (Promega, Madison, WI, USA) were cotransfected into the cells using TurboFect Transfection Reagent (Fermentas, Burlington, Canada). After 48 hours, cells were lysed, and luciferase activity was measured with Dual Luciferase Reporter Assay System (Promega) and normalized to *Renilla*. Assays were carried out in triplicate.

Statistics

All data were analyzed using IBM (Chicago, IL, USA) SPSS statistic software (version 19). $P \le .05$ was considered significant. All graphs were generated using Microsoft Excel 2010 (Microsoft Inc, Redmond, WA, USA) or GraphPad software (GraphPad Inc, La Jolla, CA, USA) (version 6).

All assays were independently repeated at least three times. Two-tailed paired *t* test was used to assess significance of all proliferation assays *in vitro*. Mann-Whitney U test was used to assess significance of assays *in vivo*. χ^2 testing was performed to evaluate Hardy-Weinberg equilibrium or deviation in the control and melanoma cases group. Conventional methods for case-control studies were used to calculate odds ratios [25], relative risks, and 95% confidence intervals (CIs) [6]. To test the significance of other data, two-tailed *t* test was used.

Results

CEACAM1 Expression Pattern in Melanoma

In light of the previously reported strong prognostic importance of CEACAM1 expression in melanoma [18], it is imperative to define its expression profile. We studied CEACAM1 expression in progression tissue microarray that includes specimens of benign nevi, primary melanoma, lymph node metastases, and remote metastases. Whereas less than 10% of the nevi faintly express cell surface CEACAM1, a gradual, prominent up-regulation was observed along disease progression, reaching 50% of the cases of remote metastases (Figure 1, *A* and *B*). This indicates that neoexpression of CEACAM1 is initiated in some of the primary tumors but commonly develops along the course of tumor progression. CEACAM1 expression was observed in two NIH-established melanoma cell lines and in four of seven

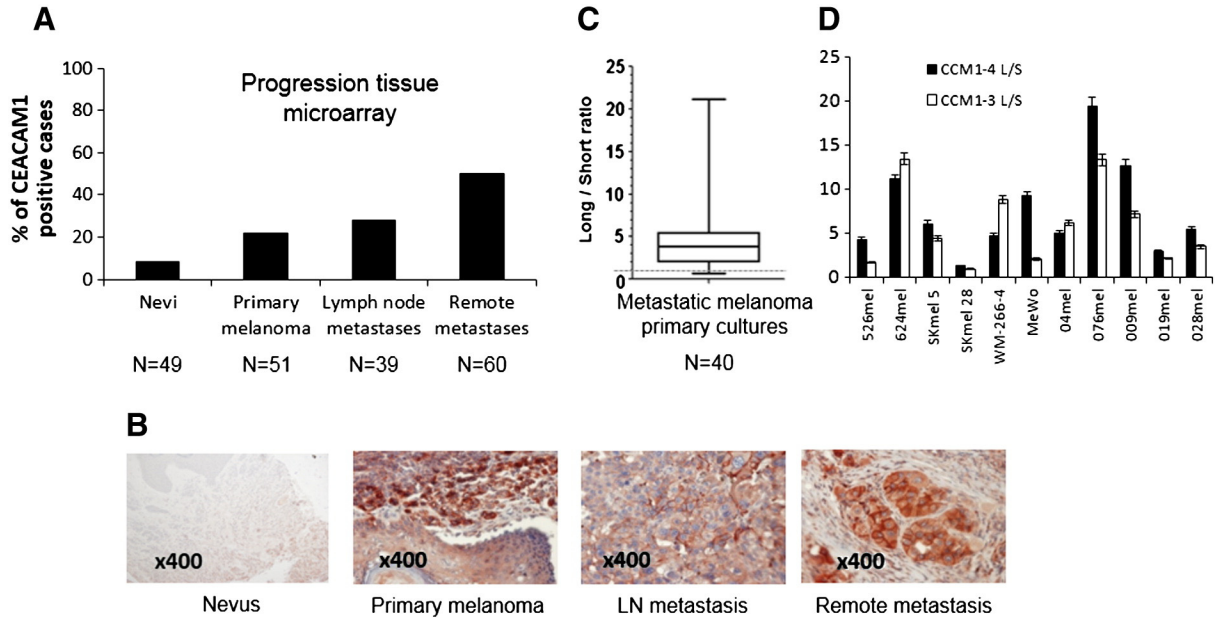

Figure 1. CEACAM1 expression during melanoma development and progression. (A) CEACAM1 expression analysis of melanoma progression tissue microarray was studied with immunohistochemistry. Figure shows the percentage of CEACAM1-positive cases. The number of tested tissues from each stage is indicated in the bottom. (B) Representative immunohistochemistry staining with MRG1 of indicated tissue cores from the tissue microarray is shown. (C) Low-passage primary cultures of metastatic melanoma cells ($n = 40$) were tested for the ratio between the long and short cytoplasmic tail CEACAM1 splice variants. Horizontal dash line represents ratio of 1. (D) Ratio between long and short forms was determined for CEACAM1 isoforms with three or four extracellular domains in melanoma cell lines. Ratios were determined with variant-specific real-time PCR.

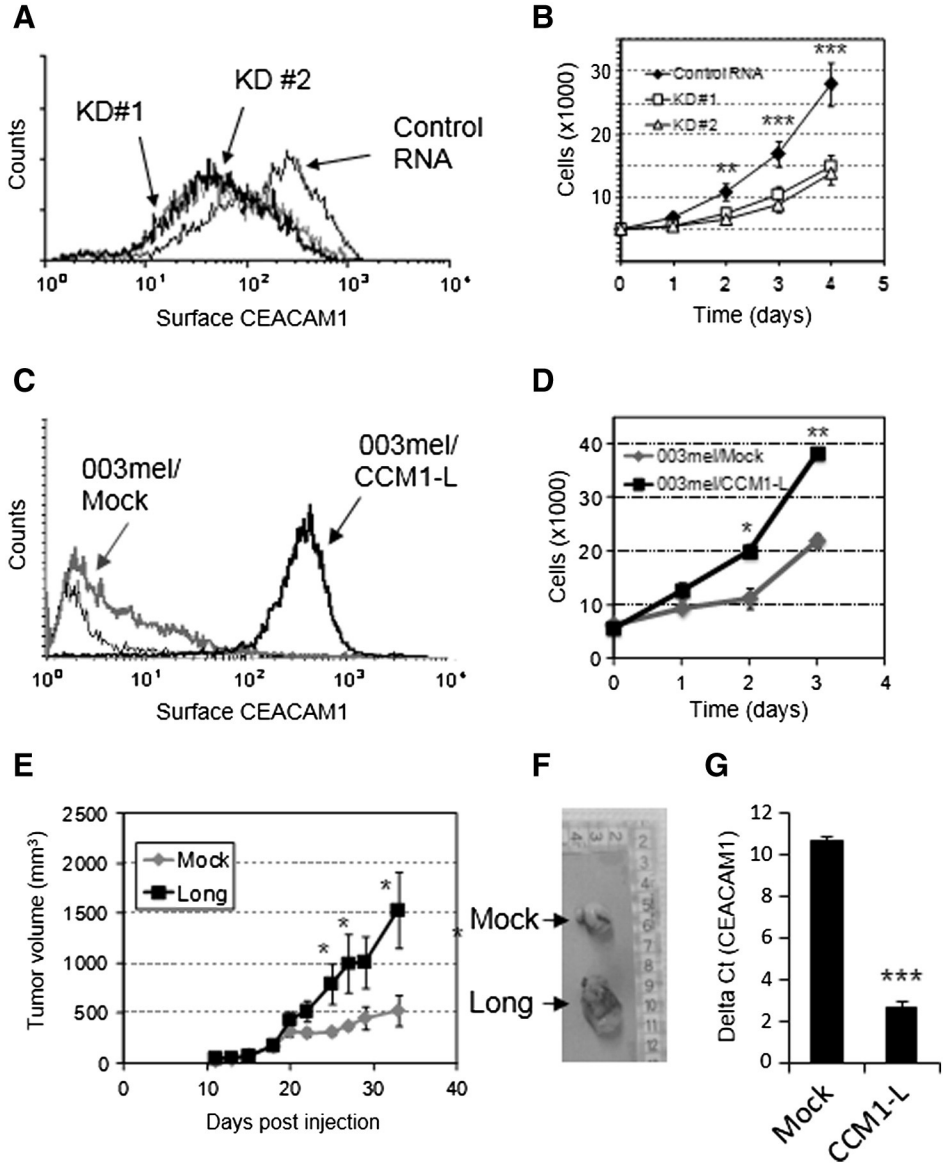

Figure 2. CEACAM1-Long facilitates melanoma cell growth. (A) Stable CEACAM1 knockdown with two different shRNA clones or scrambled sequence as control. Figure shows surface CEACAM1 expression in flow cytometry using MRG1 mAb. (B) CEACAM1-knockdown clones tested for cell proliferation, as tested with standardized XTT colorimetric assay. Figure shows a representative experiment out of three independently performed experiments. Significance was tested with paired *t* test (scramble data *vs* each clone). (C) CEACAM1-Long (CCM1-L) or empty (Mock) vectors were overexpressed in CEACAM1-negative 003mel. Figure shows surface CEACAM1 expression as tested by flow cytometry. (D) CEACAM1 overexpression or control cells were tested for proliferation with standardized XTT colorimetric assay. Figure shows a representative experiment out of three independently performed experiments. Significance was tested with paired *t* test. (E) CEACAM1 overexpression or control cells were injected subcutaneously into SCID-NOD mice. Figure shows average tumor volume measurements over time. Each group included eight animals. Figure shows a representative experiment out of three independently performed experiments. Significance was tested with Mann-Whitney U test. (F) Representative macroscopic images of extracted tumors are indicated in the figure. (G) Average CEACAM1 expression in the extracted xenografts, as tested with real-time PCR. Significance was tested with nonpaired *t* test. *Y*-axis denotes ΔC_t after normalizing to the housekeeping gene *GAPDH*. Error bars throughout the figure reflect SE. *, **, and *** denote significance values of $P < .05$, $P < .01$, and $P < .001$, respectively.

established cell lines purchased from the ATCC (Figure W1). The ratio between Long and Short CEACAM1 variants was tested with isoform-specific real-time PCR in 40 CEACAM1-positive low-passage primary cultures of metastatic melanoma. Notably, a clear dominance of the Long form was observed (Figure 1*C*). Dominance of the long cytoplasmic tail form was similarly observed in alternatively spliced isoforms containing three or four extracellular domains (Figure 1*D*).

CEACAM1 Facilitates the Proliferation of Melanoma Cells

The direct effect of CEACAM1 on the proliferation of melanoma cells was tested by selective, stable knockdown, using small hairpin RNA (shRNA) in 526mel cells. Transfection with a nontarget scrambled sequence served as negative control. The expression of CEACAM1 was decreased by 50% using two different shRNA sequences as confirmed by flow cytometry (Figure 2*A*). A significant

inhibition in the net proliferation of both knockdown clones was observed, compared to the control cells ($P < .001$; Figure 2*B*). Moreover, similar results were observed in three additional established cell lines, WM-266-4, SK mel 5, and MeWo (Figure W2, *A*–*C*). The proliferation of another established cell line, SK mel 28, was unaffected by CEACAM1 knockdown (Figure W2*D*). Complementarily, CEACAM1-negative melanoma culture 003mel was stably transfected with the CEACAM1-Long cDNA (003/CCM1-L), the dominant CEACAM1 isoform (Figure 1*C*). Transfection with an empty PQCXIP vector served as negative control (003/Mock). The expression of CEACAM1 was confirmed by flow cytometry (Figure 2*C*). In this cell system, a significant enhancement in net proliferation was observed in the CEACAM1-transfectanted cells ($P < .01$; Figure 2*D*).

The melanoma growth–promoting effect was further tested *in vivo*. Cells (003/Mock or 003/CCM1-L) were injected subcutaneously into SCID-NOD mice, which were monitored for tumor growth rates. Importantly, the average tumor growth rate of 003/CCM1-L tumors was significantly higher than that of tumors arising from injection of 003/Mock (Figure 2*E*). Extraction of all tumors after 5 weeks showed the macroscopic differences between 003/Mock and 003/CCM1-L tumors (Figure 2*F*). The expression of CEACAM1 was maintained *in vivo* (Figure 2*G*). Collectively, the combined *in vitro* and *in vivo* data strongly suggest that CEACAM1 directly enhances the proliferative potential of melanoma cells and, accordingly, their tumorigenicity.

Proliferation Is Facilitated Only By the Long Isoform of CEACAM1

In other cell systems, such as lymphocytes, it was suggested that CEACAM1 with short-tail is associated with activation, whereas the long-tail isoform is associated with inhibition [10,12,13,26]. In addition, it was reported that regulation of insulin clearance in the liver or of proliferation rate in colon cells are independent from the extracellular portion of CEACAM1 [27,28]. Therefore, the following series of constructs were made and stably transfected into the CEACAM1-negative 003mel cells: CEACAM1-Long tail (Long), CEACAM1-Short tail, CEACAM1 without a cytoplasmic tail

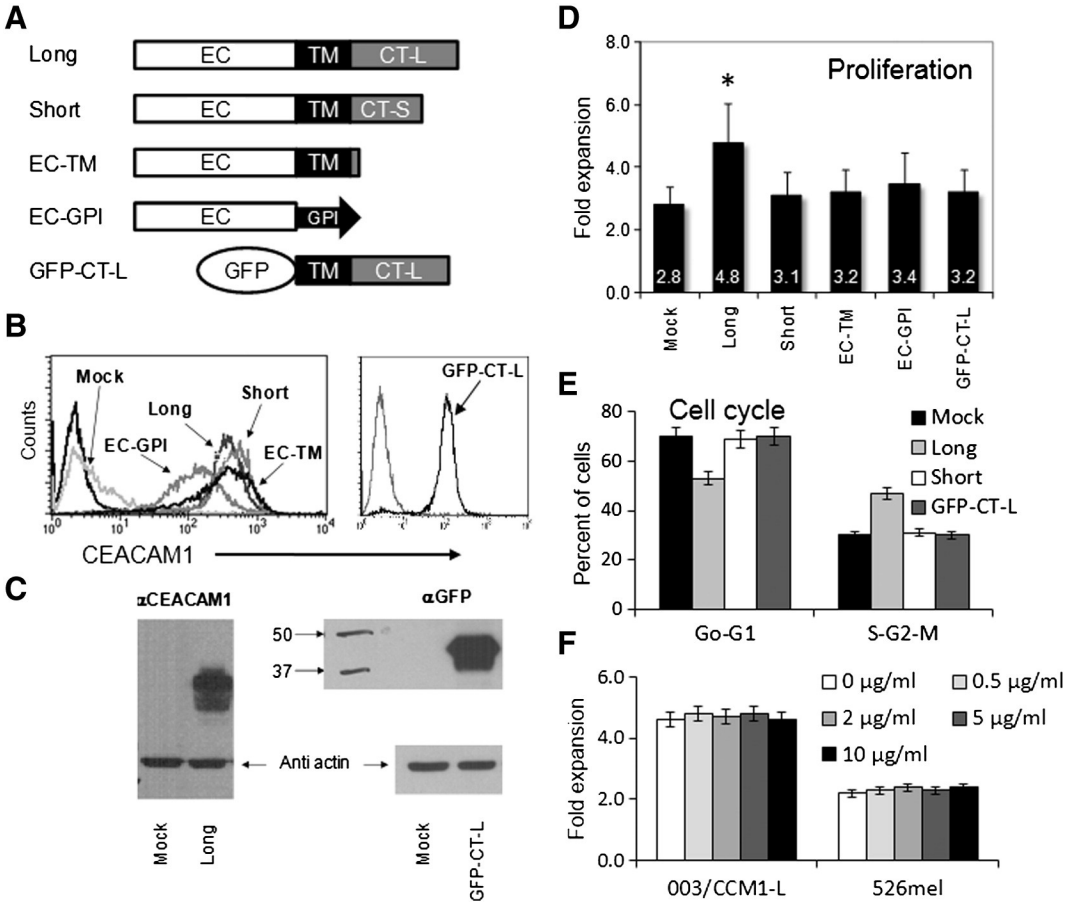

Figure 3. Defining CEACAM1 protein components required to facilitate proliferation. (A) Description of the constructs generated as indicated in the left. Long, CEACAM1-Long; Short, CEACAM1-Short; EC, extracellular; TM, transmembrane; CT-L, long cytoplasmic tail; CT-S, short cytoplasmic tail; GPI, glycosyl phosphoinositol link; GFP, green fluorescent protein. (B) All constructs were transfected into CEACAM1-negative 003mel cells. Similar expression was validated by flow cytometry for all constructs containing the extracellular portion of CEACAM1. Spontaneous fluorescence was observed for GFP-CT-L. (C) Western blot for CEACAM1 or GFP on control, Long, or GFP-CT-L cells. (D) Average proliferation fold after 2 days for each of the indicated transfectants. Proliferation was tested with standardized colorimetric XTT assay. Figure shows the average of six independent experiments. (E) Cell cycle measurements of the indicated transfectants, as measured by DNA content with flow cytometry. Cells were grouped into resting cells (G_0-G_1) or proliferating cells (S-G_2-M). Figure shows the average of three independent experiments. (F) CEACAM1-positive cells, as indicated in the figure, were incubated with various concentrations of the CEACAM1-blocking mAb MRG1 and tested for proliferation fold after 2 days with standardized colorimetric XTT assay. The figure shows the average of three independent experiments.

(EC-TM), extracellular portion of CEACAM1 fused to GPI anchor (EC-GPI), and the transmembrane with long tail portions fused downstream to GFP preceded by the leader peptide of CEACAM1 (GFP-CT-L) (Figure 3*A*). Flow cytometry using a CEACAM1-specific mAb to CEACAM1 confirmed similar expression levels of all constructs, except for the somewhat lower expression level of EC-GPI (Figure 3*B*). It is impossible to quantitatively compare the endogenous fluorescent signals of the GFP construct with the signals of the other CEACAM1 constructs, which emanate from FITC-conjugated secondary antibodies. Western blot analysis with anti-GFP confirmed that the GFP-CT-L protein was expressed similarly to CEACAM1-L (Figure 3*C*). Only the 003/CCM1-L cells displayed a consistently enhanced net proliferation compared to 003/Mock cells (Figure 3*D*). This was further supported in cell cycle analyses, which demonstrated a clear shift of almost 20% of the 003/CCM1-L cell population from resting G_0-G_1 phase to proliferating S-G_2-M phase (Figure 3*E*). Importantly, blocking of intercellular homophilic CEACAM1 interactions with a blocking mAb [17] did not inhibit the net proliferation of 526mel or 003/CCM1-L cells over a wide range of concentrations (Figure 3*F*). In conclusion, the combined results suggest that both extracellular portion and long cytosolic tail of CEACAM1 are required to enhance melanoma cell proliferation but that the mechanism may not involve homophilic intercellular CEACAM1 interactions.

CEACAM1 Enhances the Proliferation of Melanoma Cells in a Sox-2–Dependent Manner

A comparative whole-genome oligonucleotide microarray indicated that more than 650 genes were differentially expressed in a significant manner (>2- or <0.5-fold) among the 003/Mock and 003/CCM1-L cells. In agreement with the *in vitro* and *in vivo* observations (Figure 2), the most prominent functional gene clusters included cell growth and proliferation (>120 genes) and also other potentially related clusters such as cell development (about 120 genes), cell movement (about 100 genes), cell-cell interaction (about 90 genes), and other functions (Figure 4*A*). The array was successfully validated by testing several genes that were upregulated or downregulated in the 003/CCM1-L cells with real-time PCR (Figure W3).

It was recently reported that the stem cell factor Sox-2 is upregulated in melanoma as well as in some epithelial cancers [29–31]. Importantly, Sox-2 was significantly upregulated following overexpression of CEACAM1-Long both in the RNA and protein levels (Figure 4, *B* and *C*). Moreover, no similar up-regulation of Sox-2 was observed in cells transfected with CEACAM1-Short or with a construct lacking the entire extracellular portion (Figure 4*B*). This result is in agreement with the effect of CEACAM1 on proliferation (Figure 3*D*). Whereas it was previously shown that Sox-2 enhances the invasive capacity of melanoma cells [32], successful knockdown of Sox-2 in 003/CCM1-L, evident both in RNA and protein levels (Figure 4, *D* and *E*), remarkably reduced the net

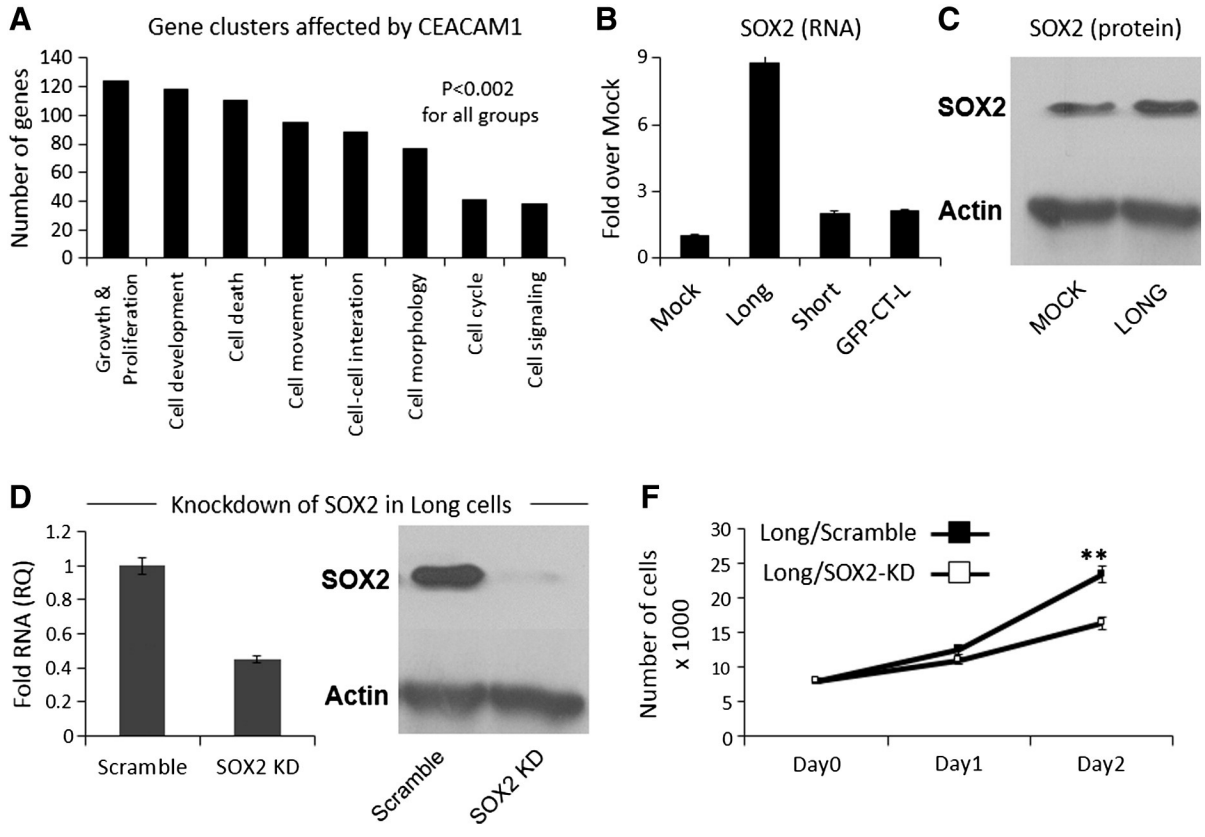

Figure 4. CEACAM1-Long enhances proliferation in a Sox-2-dependent manner. (A) Gene clusters altered in 003/Long *versus* 003/Mock cells as detected by Affymetrix oligonucleotide expression microarray. Genes were clustered according to functional groups, as indicated. *Y*-axis denotes the number of altered genes. (B) Sox-2 expression in the indicated transfectants using real-time PCR or (C) Western blot is shown. (D) Sox-2 was knocked down with small interference RNA (siRNA) in 003/Long cells, and the effect was monitored at the RNA level with real-time PCR (left) or protein level with Western blot (right). Scrambled RNAi sequence was used as control. (F) Figure shows the proliferation of 003/Long cells transfected with scrambled RNAi or Sox-2–specific RNAi using standardized colorimetric XTT assay. The figure shows a representative experiment of three experiments performed independently. Significance was tested with paired *t* test.

proliferation of these cells (Figure 4*F*). Similar results were obtained with other melanoma lines (data not shown).

Novel SNP Enhances the CEACAM1 Promoter Activity

We next analyzed the promoter of CEACAM1 for the presence of SNPs. Overall, 267 individuals were genotyped (134 patients with melanoma and 133 ethnically matched control cases). In the first genotyping assay, 75 patients with melanoma were genotyped for 14 CEACAM1 SNPs that matched the selection criteria: 3 SNPs in 5'UTR—rs41416852, rs8103285, and rs8102519; 3 SNPs in the coding region, which potentially cause missense mutations—rs8111468, rs8110904, and rs8111171; and 8 SNPs in 3'UTR—rs111284121, rs1047943a, rs14774, rs76779598, rs1047942, rs138145530, rs1047941, and rs150410858. In 12 of the 14 tested SNPs, all patients were homozygote for the common allele. The only two SNPs that showed variation in allele distribution were rs8103285 and rs8102519, located in the 5'UTR of CEACAM1. These two SNPs are near each other (62 bp) and thus are in linkage disequilibrium.

A genomic fragment upstream to the coding region of CEACAM1, which is known to carry promoter activity [33,34], was cloned upstream to luciferase reporting gene. The promoter activity was shown using IFNγ (Figure W4). To study the potential functional effect of these SNPs on the promoter activity of CEACAM1, a series of point mutations were introduced into the wild-type construct mimicking each of the SNPs separately and together. All of the constructs were cotransfected with *Renilla*-expressing vector into different melanoma cells, and normalized luciferase activity was measured. Remarkably, the wild-type promoter exhibited a significantly lower activity compared to the single and double SNP constructs in all melanoma cell lines (Figure 5*B*). Transfection of an empty vector with no promoter upstream to the luciferase hardly produced measurable signals (Figure 5*B*). This observation strongly indicates that these SNPs enhance the promoter activity of CEACAM1. Both SNPs contribute to this enhanced activity, but the genetically relevant construct is the double SNP, as these SNPs occur together being in linkage disequilibrium.

Germ Line Genotype Carrying the Double SNP in the CEACAM1 Promoter Enhances the Risk to Develop Melanoma

To evaluate the medical relevance of the promoter enhancing SNPs, we tested their frequency in the germ line of 134 patients with melanoma and in 133 ethnically matched healthy controls. In the control group, the SNPs displayed no deviation from Hardy-Weinberg equilibrium; however, the patients with melanoma showed a statistically significant deviation, suggesting an association between these SNPs in CEACAM1 5'UTR and melanoma phenotype. Results show an association between melanoma and homozygosity to the rare alleles of SNPs rs8103285 and rs8102519, with an allelic Odds Ratio (OR) of 2.05 (95% CI = 0.86-0.49; P = .1). Remarkably, homozygosity to these alleles conferred increased risk to melanoma with relative risk of 1.35 (95% CI = 1.01-1.81; P = .05).

Discussion

Expression analysis in various types of cancer shows that CEACAM1 is overexpressed in some malignancies, such as melanoma, lung cancer, and thyroid carcinoma, whereas it is downregulated in colon, prostate, endometrial, and breast cancers [35]. CEACAM1 exerts tumor-suppressive effects in colon [21], prostate [22], and breast cancer cells [36], which could explain its loss in these types of cancers. However, in melanoma and lung cancer, the presence of CEACAM1 is known to strongly predict the development of aggressive disease with poor outcome [18,37,38]. The only mechanistic explanation potentially accounting for this clinical observation was that CEACAM1 directly inhibits activated NK and T lymphocytes [8,15,18,37,38]. There was no information regarding the direct effects of CEACAM1 on melanoma cells.

Here, we found that CEACAM1 is gradually upregulated along melanoma development and progression (Figure 1), as opposed to the acquired mutation in BRAF, which is observed already at the stage of nevus [39]. Analysis of metastatic melanoma cultures shows predominance of the CEACAM1-Long tail (Figure 1). Knockdown or overexpression of CEACAM1-Long directly led to inhibition or facilitation of proliferation *in vitro*, respectively. CEACAM1-Long overexpression further facilitated *in vivo* xenograft tumorigenicity of melanoma (Figure 2). Thus, CEACAM1 has a dual role in melanoma, as it provides direct protection from late effector lymphocytes [8,15] and exerts oncogenic effects. This is in line with the gradual up-regulation along disease progression.

CEACAM1 inhibits proliferation of colon cancer cells even *in the absence* of its entire extracellular domain [27]. Similarly, CEACAM1 regulates insulin clearance by cytoplasmic tail interactions with insulin receptor [40]. Conversely, homophilic intercellular interactions are the cornerstone of lymphocyte inhibition by CEACAM1 [8,13,15], which can be targeted with mAbs [17]. By employing a cell system of CEACAM1 truncated mutants, we positively show that both the

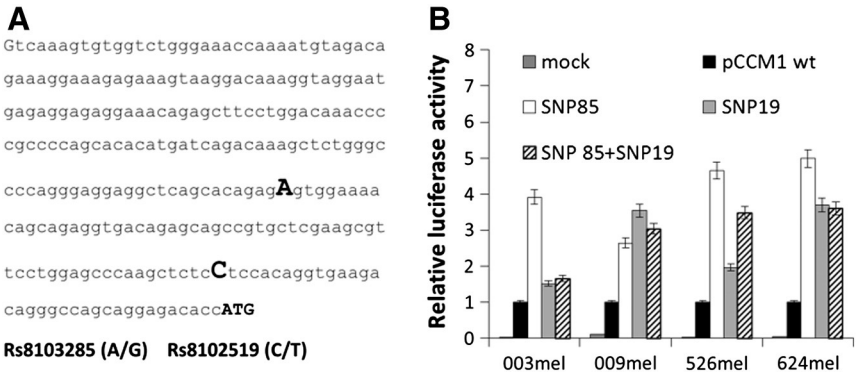

Figure 5. Functional SNPs in the promoter of CEACAM1. (A) Part sequence of the CEACAM1 promoter. ATG and the location of the studied SNPs are bolded and enlarged. (B) Functional fragments of the CEACAM1 promoter carrying the consensus nucleotides (pCCM1 WT), each SNP (SNP85 or SNP19), or both (SNP85 + SNP19) were cloned upstream to a luciferase reporter. Empty vector (Mock) or promoter constructs were transfected and tested for luciferase activity in various melanoma cell lines, as indicated. The activity of the wild-type promoter was set as the point of reference. Figure shows an average of three independent experiments performed.

extracellular and the long cytoplasmic tail are required to enhance melanoma cell proliferation (Figure 3). Interestingly, antibodies that block the N-domain of CEACAM1 failed to affect proliferation (Figure 3). CEACAM1 is known to bind heterotypically to CEACAM5 [41] or to various bacterial proteins [7], none of which are found in melanoma cells. However, it was previously shown that CEACAM1 exerts *cis*-interactions with integrins, such as integrin β3, as previously reported [42]. Preclinical studies with anti–integrin $\alpha_v\beta_3$ mAb reported on inhibition of tumor proliferation [43]. It is still unclear whether this integrin is an effector of CEACAM1 in enhancing melanoma cell proliferation. The protein partner of CEACAM1 enabling the facilitation of proliferation in melanoma cells remains to be identified.

The up-regulation of CEACAM1-Long in melanoma cells triggers the expression of many functional gene groups that are associated with the observed phenotype (Figures 3 and 4). Sox-2, which was upregulated by CEACAM1-Long at the RNA and protein levels, was proven instrumental in enhancing the proliferation of melanoma cells (Figure 4). Sox-2 is one of the Yamanaka factors associated with induction of inducible pluripotent stem cells [44]. The role of Sox-2 was very limitedly investigated in melanoma cells. Previously reported expression analyses demonstrated a gradual up-regulation from 14% in nevi and up to 80% in metastatic melanoma [30], which resembles the expression profile of CEACAM1 (Figure 1). In addition, it was shown that Sox-2 enhances the invasive capacity of melanoma cell [32]. Interestingly, Sox-2 enhances metastasis of breast and prostate cancer cells by promoting of WNT/β-catenin signaling. Dual luciferase assay and chromatin immunoprecipitation revealed activation and binding of Sox-2 to the promoter region of β-catenin [45]. Recently, it was identified that Armadillo repeats of β-catenin binds to the H469 and K470 in the cytoplasmic domain of CEACAM1 long cytoplasmic tail [46], which enables redistribution of β-catenin to the cytoskeleton and inhibition of its degradation [47]. We speculate that, in melanoma, CEACAM1 overexpression and the subsequently induced Sox-2 culminate in enhanced expression of β-catenin by Sox-2 and its protection from degradation by the long cytoplasmic tail of CEACAM1. Indeed, the Wnt/β-catenin pathway is overactive in melanoma, facilitating oncogenic and chemoresistant properties [48]. The postulated role of CEACAM1 and Sox-2 in activating Wnt/β-catenin pathway in melanoma remains to be tested.

To delineate factors contributing to the increased CEACAM1 expression in melanoma, we studied its promoter. Bioinformatics analysis pointed on a hypothetical M-Box for MITF in the promoter. However, we failed to positively show any regulation of CEACAM1 promoter by MITF-M (data not shown). SNP analysis pointed on two extremely close positions upstream to the ATG; each significantly enhances its activity in melanoma cells (Figure 5). Due to the close proximity, they are inherited together. Sequencing of 134 germ-line DNA samples derived from patients with melanoma and 133 samples from matched healthy donors reveals that, whereas the healthy donor population complies with the Hardy-Weinberg equilibrium, the population of the patients with melanoma deviates from it significantly, attesting for an association between these SNPs and melanoma. Moreover, germ-line homozygosity increases the chances to develop melanoma by 35% (Table 1). This observation is consistent with the enhanced promoter activity conferred by these SNPs (Figure 5), which could lower the threshold for CEACAM1 expression, and thereby enhance proliferation and immune evasion effects. It is still unclear why these SNPs increase the promoter activity. One possibility could be alteration of putative binding sites for transcription factors or repressors.

Table 1. SNP Distribution in Patients with Melanoma and Healthy Donors

	Patients with Melanoma	Healthy Donors
	N = 134	*N* = 133
Genotype	Counts	
Consensus nucleotides	94 (70.1%)	83 (62.4%)
Double SNPs, heterozygote	32 (23.9%)	46 (34.6%)
Double SNPs, homozygote	8 (6%)	4 (3%)
χ^2	4.73	0.63
Hardy-Weinberg equilibrium	No	Yes

The overall frequencies of rs8103285 and rs8102519 in a cohort of 134 patients with melanoma and 133 healthy donors are displayed. Hardy-Weinberg equilibrium (χ^2) of population of both groups was calculated groups using the conventional method.

By employing predictive tools, such as PROMO [49], new putative binding sites for various transcription factors, such as signal transducer and activator 4 (STAT4), ETS1-v-ets avian erythroblastosis virus E26 oncogene homolog 1, and ELK-1, are generated by these SNPs. Thus, the SNP genotype in the promoter of CEACAM1 is not just a statistical marker for enhanced risk but also rather reflects a mechanism. At the moment, there are only a few genetic markers for enhanced risk to develop melanoma: cyclin-dependent kinase inhibitor 2A (CDKN2A), cyclin-dependent kinase 4 (CDK4), The melanocortin 1 receptor (MC1R), and some other low-risk markers such as tyrosinase (TYR), vitamin D receptor (VDR), and HLA-DQB0301 [50]. CEACAM1 genotyping might be used in the future to identify high-risk populations, but first, these findings must be validated in larger cohorts.

Supplementary data to this article can be found online at http://dx.doi.org/10.1016/j.neo.2014.05.003.

Acknowledgments

The authors thank Michael Aaronson, Nehemia, and Haya Lemelbaum for their generous and continuous support. The authors also thank Nira Koren-Morag (Department of Epidemiology and Statistics, Sackler Faculty of Medicine, Tel Aviv University) for her counseling on statistics.

This work was conducted in partial fulfillment of the requirements for PhD degree of R.O., Sackler Faculty of Medicine, Tel Aviv University.

References

[1] Siegel R, Naishadham D, and Jemal A (2013). Cancer statistics, 2013. *CA Cancer J Clin* **63**, 11–30.
[2] Miller AJ and Mihm Jr MC (2006). Melanoma. *N Engl J Med* **355**, 51–65.
[3] Gajewski TF (2007). Failure at the effector phase: immune barriers at the level of the melanoma tumor microenvironment. *Clin Cancer Res* **13**, 5256–5261.
[4] Sang M, Wang L, Ding C, Zhou X, Wang B, Lian Y, and Shan B (2011). Melanoma-associated antigen genes - an update. *Cancer Lett* **302**, 85–90.
[5] Flaherty KT, Robert C, Hersey P, Nathan P, Garbe C, Milhem M, Demidov LV, Hassel JC, Rutkowski P, and Mohr P, et al (2012). Improved survival with MEK inhibition in BRAF-mutated melanoma. *N Engl J Med* **367**, 107–114.
[6] Robert C, Thomas L, Bondarenko I, O'Day S, Weber J, Garbe C, Lebbe C, Baurain JF, Testori A, and Grob JJ, et al (2011). Ipilimumab plus dacarbazine for previously untreated metastatic melanoma. *N Engl J Med* **364**, 2517–2526.
[7] Gray-Owen SD and Blumberg RS (2006). CEACAM1: contact-dependent control of immunity. *Nat Rev Immunol* **6**, 433–446.
[8] Markel G, Gruda R, Achdout H, Katz G, Nechama M, Blumberg RS, Kammerer R, Zimmermann W, and Mandelboim O (2004). The critical role of residues ^{43}R and ^{44}Q of carcinoembryonic antigen cell adhesion molecules-1 in the protection from killing by human NK cells. *J Immunol* **173**, 3732–3739.
[9] Sapoznik S, Ortenberg R, Schachter J, and Markel G (2012). CEACAM1 in malignant melanoma: a diagnostic and therapeutic target. *Curr Top Med Chem* **12**, 3–10.
[10] Morales VM, Christ A, Watt SM, Kim HS, Johnson KW, Utku N, Texieira AM, Mizoguchi A, Mizoguchi E, and Russell GJ, et al (1999). Regulation of human

intestinal intraepithelial lymphocyte cytolytic function by biliary glycoprotein (CD66a). *J Immunol* **163**, 1363–1370.
[11] Boulton IC and Gray-Owen SD (2002). Neisserial binding to CEACAM1 arrests the activation and proliferation of CD4$^+$ T lymphocytes. *Nat Immunol* **3**, 229–236.
[12] Markel G, Wolf D, Hanna J, Gazit R, Goldman-Wohl D, Lavy Y, Yagel S, and Mandelboim O (2002). Pivotal role of CEACAM1 protein in the inhibition of activated decidual lymphocyte functions. *J Clin Invest* **110**, 943–953.
[13] Markel G, Lieberman N, Katz G, Arnon TI, Lotem M, Drize O, Blumberg RS, Bar-Haim E, Mader R, and Eisenbach L, et al (2002). CD66a interactions between human melanoma and NK cells: a novel class I MHC-independent inhibitory mechanism of cytotoxicity. *J Immunol* **168**, 2803–2810.
[14] Markel G, Mussaffi H, Ling KL, Salio M, Gadola S, Steuer G, Blau H, Achdout H, de Miguel M, and Gonen-Gross T, et al (2004). The mechanisms controlling NK cell autoreactivity in TAP2-deficient patients. *Blood* **103**, 1770–1778.
[15] Markel G, Seidman R, Stern N, Cohen-Sinai T, Izhaki O, Katz G, Besser M, Treves AJ, Blumberg RS, and Loewenthal R, et al (2006). Inhibition of human tumor-infiltrating lymphocyte effector functions by the homophilic carcinoembryonic cell adhesion molecule 1 interactions. *J Immunol* **177**, 6062–6071.
[16] Besser MJ, Shapira-Frommer R, Treves AJ, Zippel D, Itzhaki O, Schallmach E, Kubi A, Shalmon B, Hardan I, and Catane R, et al (2009). Minimally cultured or selected autologous tumor-infiltrating lymphocytes after a lympho-depleting chemotherapy regimen in metastatic melanoma patients. *J Immunother* **32**, 415–423.
[17] Ortenberg R, Sapir Y, Raz L, Hershkovitz L, Ben Arav A, Sapoznik S, Barshack I, Avivi C, Berkun Y, and Besser MJ, et al (2012). Novel immunotherapy for malignant melanoma with a monoclonal antibody that blocks CEACAM1 homophilic interactions. *Mol Cancer Ther* **11**, 1300–1310.
[18] Thies A, Moll I, Berger J, Wagener C, Brummer J, Schulze HJ, Brunner G, and Schumacher U (2002). CEACAM1 expression in cutaneous malignant melanoma predicts the development of metastatic disease. *J Clin Oncol* **20**, 2530–2536.
[19] Markel G, Ortenberg R, Seidman R, Sapoznik S, Koren-Morag N, Besser MJ, Bar J, Shapira R, Kubi A, and Nardini G, et al (2010). Systemic dysregulation of CEACAM1 in melanoma patients. *Cancer Immunol Immunother* **59**, 215–230.
[20] Thies A, Mauer S, Fodstad O, and Schumacher U (2007). Clinically proven markers of metastasis predict metastatic spread of human melanoma cells engrafted in scid mice. *Br J Cancer* **96**, 609–616.
[21] Fournès B, Sadekova S, Turbide C, Létourneau S, and Beauchemin N (2001). The CEACAM1-L Ser503 residue is crucial for inhibition of colon cancer cell tumorigenicity. *Oncogene* **20**, 219–230.
[22] Busch C, Hanssen T, Wagener C, and OBrink B (2002). Down-regulation of CEACAM1 in human prostate cancer: correlation with loss of cell polarity, increased proliferation rate, and Gleason grade 3 to 4 transition. *Hum Pathol* **33**, 290–298.
[23] Heckman K and Pease L (2007). Gene splicing and mutagenesis by PCR-driven overlap extension. *Nat Protoc* **2**, 924–932.
[24] Ragoussis J, Elvidge GP, Kaur K, and Colella S (2006). Matrix-assisted laser desorption/ionisation, time-of-flight mass spectrometry in genomics research. *PLoS Genet* **2**, e100.
[25] Chen L, Chen Z, Baker K, Halvorsen EM, da Cunha AP, Flak MB, Gerber G, Huang YH, Hosomi S, and Arthur JC, et al (2012). The short isoform of the CEACAM1 receptor in intestinal T cells regulates mucosal immunity and homeostasis *via* Tfh cell induction. *Immunity* **37**, 930–946.
[26] Nakajima A, Iijima H, Neurath MF, Nagaishi T, Nieuwenhuis EE, Raychowdhury R, Glickman J, Blau DM, Russell S, and Holmes KV, et al (2002). Activation-induced expression of carcinoembryonic antigen-cell adhesion molecule 1 regulates mouse T lymphocyte function. *J Immunol* **168**, 1028–1035.
[27] Izzi L, Turbide C, Houde C, Kunath T, and Beauchemin N (1999). *cis*-Determinants in the cytoplasmic domain of CEACAM1 responsible for its tumor inhibitory function. *Oncogene* **18**, 5563–5572.
[28] Poy MN, Ruch RJ, Fernstrom MA, Okabayashi Y, and Najjar SM (2002). Shc and CEACAM1 interact to regulate the mitogenic action of insulin. *J Biol Chem* **277**, 1076–1084.
[29] Bernhardt M, Galach M, Novak D, and Utikal J (2012). Mediators of induced pluripotency and their role in cancer cells – current scientific knowledge and future perspectives. *Biotechnol J* **7**, 810–821.
[30] Chen PL, Chen W-S, Li J, Lind AC, and Lu D (2013). Diagnostic utility of neural stem and progenitor cell markers nestin and SOX2 in distinguishing nodal melanocytic nevi from metastatic melanomas. *Mod Pathol* **26**, 44–53.
[31] Xiang R, Liao D, Cheng T, Zhou H, Shi Q, Chuang TS, Markowitz D, Reisfeld RA, and Luo Y (2011). Downregulation of transcription factor SOX2 in cancer stem cells suppresses growth and metastasis of lung cancer. *Br J Cancer* **104**, 1410–1417.
[32] Girouard SD, Laga AC, Mihm MC, Scolyer RA, Thompson JF, Zhan Q, Widlund HR, Lee C-W, and Murphy GF (2012). SOX2 contributes to melanoma cell invasion. *Lab Invest* **92**, 362–370.
[33] Chen C-J, Lin TT, and Shively JE (1996). Role of interferon regulatory factor-1 in the induction of biliary glycoprotein (cell CAM-1) by interferon-γ. *J Biol Chem* **271**, 28181–28188.
[34] Phan D, Cheng CJ, Galfione M, Vakar-Lopez F, Tunstead J, Thompson NE, Burgess RR, Najjar SM, Yu-Lee LY, and Lin SH (2004). Identification of Sp2 as a transcriptional repressor of carcinoembryonic antigen-related cell adhesion molecule 1 in tumorigenesis. *Cancer Res* **64**, 3072–3078.
[35] Obrink B (2008). On the role of CEACAM1 in cancer. *Lung Cancer* **60**, 309–312.
[36] Luo W, Wood C, Earley K, Hung M, and Lin S (1997). Suppression of tumorigenicity of breast cancer cells by an epithelial cell adhesion molecule (C-CAM1): the adhesion and growth suppression are mediated by different domains. *Oncogene* **14**, 1697–1704.
[37] Laack E, Nikbakht H, Peters A, Kugler C, Jasiewicz Y, Edler L, Brummer J, Schumacher U, and Hossfeld DK (2002). Expression of CEACAM1 in adenocarcinoma of the lung: a factor of independent prognostic significance. *J Clin Oncol* **20**, 4279–4284.
[38] Sienel W, Dango S, Woelfle U, Morresi-Hauf A, Wagener C, Brümmer J, Mutschler W, Passlick B, and Pantel K (2003). Elevated expression of carcinoembryonic antigen-related cell adhesion molecule 1 promotes progression of non-small cell lung cancer. *Clin Cancer Res* **9**, 2260–2266.
[39] Uribe P, Wistuba II, and González S (2003). BRAF mutation: a frequent event in benign, atypical, and malignant melanocytic lesions of the skin. *Am J Dermatopathol* **25**, 365–370.
[40] Poy MN, Yang Y, Rezaei K, Fernström MA, Lee AD, Kido Y, Erickson SK, and Najjar SM (2002). CEACAM1 regulates insulin clearance in liver. *Nat Genet* **30**, 270–276.
[41] Oikawa S, Kuroki M, Matsuoka Y, Kosaki G, and Nakazato H (1992). Homotypic and heterotypic Ca^{++}-independent cell adhesion activities of biliary glycoprotein, a member of carcinoembryonic antigen family, expressed on CHO cell surface. *Biochem Biophys Res Commun* **186**, 881–887.
[42] Brümmer J, Ebrahimnejad A, Flayeh R, Schumacher U, Löning T, Bamberger AM, and Wagener C (2001). *cis* Interaction of the cell adhesion molecule CEACAM1 with integrin β_3. *Am J Pathol* **159**, 537–546.
[43] Hersey P, Sosman J, O'Day S, Richards J, Bedikian A, Gonzalez R, Sharfman W, Weber R, Logan T, and Buzoianu M, et al (2010). A randomized phase 2 study of etaracizumab, a monoclonal antibody against integrin $\alpha_v\beta_3$, ± dacarbazine in patients with stage IV metastatic melanoma. *Cancer* **116**, 1526–1534.
[44] Yamanaka S (2008). Induction of pluripotent stem cells from mouse fibroblasts by four transcription factors. *Cell Prolif* **41**, 51–56.
[45] Li X, Xu Y, Chen Y, Chen S, Jia X, Sun T, Liu Y, Li X, Xiang R, and Li N (2013). SOX2 promotes tumor metastasis by stimulating epithelial-to-mesenchymal transition via regulation of WNT/β-catenin signal network. *Cancer Lett* **336**, 379–389.
[46] Jin L, Li Y, Chen CJ, Sherman MA, Le K, and Shively JE (2008). Direct interaction of tumor suppressor CEACAM1 with Beta catenin: identification of key residues in the long cytoplasmic domain. *Exp Biol Med* **233**, 849–859.
[47] Li Y and Shively JE (2013). CEACAM1 regulates Fas-mediated apoptosis in Jurkat T-cells *via* its interaction with β-catenin. *Exp Cell Res* **319**, 1061–1072.
[48] Hartman ML and Czyz M (2013). Anti-apoptotic proteins on guard of melanoma cell survival. *Cancer Lett* **331**, 24–34.
[49] http://alggen.lsi.upc.es/cgi-bin/promo_v3/promo/promoinit.cgi?dirDB=TF_8.3.
[50] Ward KA, Lazovich D, and Hordinsky MK (2012). Germline melanoma susceptibility and prognostic genes: a review of the literature. *J Am Acad Dermatol* **67**, 1055–1067.